

# Observing exoplanets with the MicroObservatory: 43 new transit light curves of the hot Jupiter HAT-P-32b

Martin J. F. Fowler, Frank F. Sienkiewicz, Robert T. Zellem & Mary E. Dussault

Observations of 43 complete transits of the hot Jupiter exoplanet HAT-P-32b using the MicroObservatory 0.15m robotic telescope network, covering a period of seven years, are presented. Compared with the most recent ephemeris for the system, the precision of the mid-transit times yields a root-mean-square value from the predicted model of 3.0min. The estimated system parameters based on EXOFAST modelling are broadly consistent with the default parameter values listed in the NASA Exoplanet Archive. An updated orbital period of  $2.15000815 \pm 0.00000013$ d and ephemeris of  $2458881.71392 \pm 0.00027$ BJD<sub>TDB</sub> are consistent with recent studies of the system using larger telescopes. Using this updated ephemeris, the predicted mid-transit time for a notional observation of HAT-P-32b by the NASA JWST mission in mid-2021 is improved by 1.4min compared with the discovery ephemeris and is approximately eight times more precise. Likewise, the mid-transit time for an observation by the ESA ARIEL mission in 2020 is improved by 1.7min. Thus, observations of transiting exoplanets by MicroObservatory and other users of small telescopes can contribute to the maintenance of the ephemerides of targets for future space-based telescope missions. We also note that one of the HAT-P-32 field stars is a delta Scuti pulsating variable and that characterisation using the same observations as this study further demonstrates the utility of MicroObservatory for the observation of stellar variability, whilst simultaneously observing transiting exoplanets for ephemeris maintenance.

## Introduction

Over two decades on from the discovery of the first planet orbiting a main-sequence star other than our own Sun,<sup>1</sup> the number of confirmed exoplanets in the NASA Exoplanet Archive as of 2020 May 21 was 4,158, with a similar number of candidates awaiting confirmation.<sup>2,3</sup> The diversity of such worlds spans a much wider range of physical conditions than those in our solar system and form a continuum, from gas giants composed mostly of hydrogen, to smaller ocean planets where water may provide most of the mass, to rock-iron terrestrial worlds in some ways similar to the Earth.<sup>4</sup> One particular group of exoplanets with no solar-system counterpart is known as the ‘hot Jupiters’ class. These planets have masses comparable to, or greater than, Jupiter but orbit very close to their primary star (*i.e.*, within 0.1au). Exoplanets appear to be ubiquitous and it is estimated that for the stars that have been searched most thoroughly, *i.e.*, main-sequence dwarfs of 0.5–1.0 solar masses ( $M_{\odot}$ ), the probability that a random star has a planet is of the order of unity.<sup>5</sup>

Under the fortuitous condition that the orbital plane of a planetary system is coincident with the observer’s line of sight, exoplanets can be observed to transit their host star, leading to a periodic slight dimming of the star.<sup>6</sup> Known as the ‘transit method’, this technique has been used to great effect by ground-based observatories such as the Hungarian-made Automated Telescope Network (HATNet),<sup>7</sup> and the Wide Angle Search for Planets (WASP),<sup>8</sup> as well as the space-based missions *CoRoT*, *Kepler* and, currently, the *Transiting Exoplanet Survey Satellite* (TESS).<sup>9</sup> To date, *Kepler* has been responsible for the discovery of most of the known exoplanets,<sup>10</sup> and TESS is predicted to discover >10,000 new transiting examples.<sup>11</sup>

Relatively modest equipment, such as a 0.25m Schmidt–Cassegrain telescope on an equatorial mount, can be used by amateur astronomers to yield high-precision transit light curves of hot-Jupiter exoplanets.<sup>12</sup> The Exoplanet Transit Database (ETD), run by the Czech Astronomical Society,<sup>13</sup> currently includes data on >9,500 transits of over 350 exoplanets, the majority contributed by amateur observers. Amateur data from the ETD and other sources have been used to investigate transit timing variations,<sup>14,15</sup> as well as for the refinement of ephemerides of transiting exoplanets with high timing uncertainties.<sup>16</sup>

Indeed, observations of transiting exoplanets by amateurs and other users of small telescopes ( $\leq 1$ m), have an important role to play in the maintenance of the ephemerides of targets for future space-based telescope missions.<sup>17,18</sup> These missions include the NASA *James Webb Space Telescope* (JWST, 2021 launch), the ESA ARIEL mission (2028 launch), and an Astro2020 Decadal mission ( $\sim 2030$  launch). Without follow-up by ground-based observations, the ephemerides of many of these targets would become ‘stale’ by the time the missions are flown, leading to the prospect of inefficient use of valuable telescope time because of the uncertainty in the transit timings. To this end, projects such as NASA Exoplanet Watch and ARIEL ExoClock,<sup>17,19,20,21</sup> both of which are open to amateur observers and other users of small telescopes, have been established to monitor transiting exoplanets in order to keep their ephemerides up to date.

Observations of transiting exoplanets also form the basis of the Laboratory for the Study of Exoplanets (ExoLab), an online teaching resource that is operated by the Science Education Department at the Center for Astrophysics, Harvard & Smithsonian.<sup>22,23</sup> Developed with funding from the US National Science Foundation, and aimed at high-school classrooms in physics, astronomy

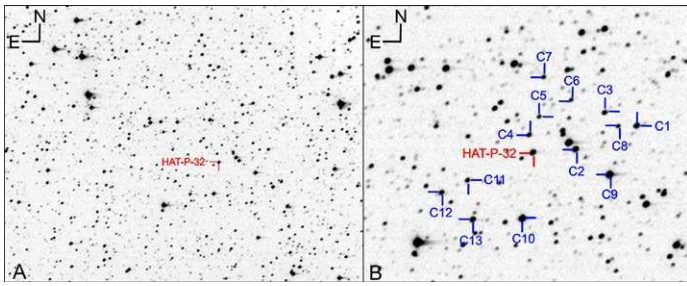


**Figure 1.** (A) Representative unfiltered full-frame MicroObservatory image of the HAT-P-32 field acquired on 2020 Jan 18. (B) Enlargement, showing the comparison stars used for aperture photometry (identified as C1 through C13).

and Earth science, ExoLab uses the 6-inch (152mm) telescopes of the MicroObservatory robotic telescope network to enable students to detect and analyse the transits of known exoplanets using rudimentary online photometry and modelling tools. Since 2009, MicroObservatory has taken >3,500 transit datasets to serve science students and interested exoplanet observers.

Complementing ExoLab, the ‘DIY Planet Search’ website – a project of NASA’s Universe of Learning<sup>24,25</sup> – is a public engagement tool that uses the same image data as ExoLab and allows anyone to investigate the transit method. Whilst a similar online photometry tool is provided on the website, the images can be downloaded as FITS files for offline reduction and analysis.<sup>26</sup> Importantly, these are all new observations; over the course of a year many are made of around 30 known exoplanets.

One of the targets regularly observed by DIY Planet Search is the  $V = 11.3$ mag, late-F–early-G dwarf star GSC 3281-00800 (= HAT-P-32), which is orbited by the exoplanet HAT-P-32b. Discovered by the HATNet in 2004 and confirmed some seven years later, HAT-P-32b was initially found to have a mass of  $\sim 0.86M_J$ , radius of  $\sim 1.789R_J$ , transit depth of the order of 20 millimagnitudes and an orbital period,  $P$ , of  $\sim 2.15$ d.<sup>27</sup> The mass and radius estimates were subsequently refined to  $0.68M_J$  and  $1.98R_J$  respectively.<sup>28</sup> The planet’s dayside temperature has been measured by Zhao *et al.* (2014) to be  $T_{eq} = 2,042 \pm 50$ K,<sup>29</sup> and its optical transmission spectrum shows little variation, suggesting a high-altitude cloud layer masking any atmospheric features.<sup>30–33</sup> Seeliger *et al.* (2014) have shown from transit timing analysis that the HAT-P-32 system does not exhibit transit timing variations (TTVs), arising from additional unknown bodies, of more than  $\sim 1.5$ min,<sup>34</sup> making it a good target to evaluate the accuracy and suitability of MicroObservatory observations for exoplanet research.

In this paper, we present observations of 43 transits of exoplanet HAT-P-32b by the MicroObservatory together with estimates of the parameters of the system based on the analysis of combined transit light curves, and an updated ephemeris.

## Observations

Between 2013 and 2020, 43 complete transits by HAT-P-32b were successfully observed by the MicroObservatory robotic telescopes (Table 1). During this period, observations of a further 40 transit events were attempted, of which 11 provided partial transits and the remainder were unsuccessful either because of: technical issues (10); poor weather (14); or very noisy transits that could not be analysed successfully (5). Overall, the success rate of observing complete HAT-P-32b transits was  $\sim 52\%$ .

Except for the observations of 2014 Oct 4, which were made using the MicroObservatory telescope *Donald*, all the observations were made with the telescope *Cecilia*.<sup>35</sup> Located at the Smithsonian’s Fred Lawrence Whipple Observatory (FLWO) in Amado, Arizona, USA, the MicroObservatory telescopes are of an original Maksutov design, with a 6-inch [152mm] spherical primary mirror and a focal length of 560mm.<sup>22</sup> A Kodak KAF-1402ME CCD sensor produces images covering a field of view of  $0.96 \times 0.75^\circ$ , with a nominal plate scale of 5.21 arcsec/pixel ( $2 \times 2$  binning). For each observation run, we obtained unfiltered 60s-exposure science FITS images with a three-minute cadence, from around one hour before and one hour after the predicted start/end of the transit, giving approximately 100 images per run. The headers of the FITS images were time-stamped with the start of exposure based on a local precise time server at the FLWO and are accurate to the nearest second.

In addition to the science images, two dark-field images were collected on each run. Whilst flat-field (FF) images were not available, for the 2016 runs which were particularly noisy with dust motes, a master pseudo-FF was prepared from nine images of the exoplanetary system WASP-52, obtained on an overcast moonlit night. This pseudo-FF to some extent offset the ‘wandering’ of the target and comparison stars across the sensor throughout the sequence of images, although this remains a significant source of noise in the datasets. A representative science image showing the HAT-P-32 field is shown in Figure 1.

## Data reduction & analysis pipeline

We developed a partially automated MicroObservatory Exoplanet Observation Workflow pipeline (*MEOW* v. 1.0) for reduction and analysis of the DIY Planet Search images. For each set of observations, the science images, together with a dark-field image and, where available, the pseudo-FF image, were imported into *MuniWin* (v. 2.1.24 ( $\times 64$ )),<sup>36</sup> for automated differential aperture photometry using an ensemble of up to eight comparison stars as shown in Figure 1 and detailed in Table 1. The measuring aperture was typically three pixels in radius and the background sky was measured using a concentric aperture of two pixels, with a gap of one pixel between the two apertures. We then saved the photometry output from *MuniWin* (Julian Date ( $JD_{UTC}$ ) of mid-observation,  $V-C$  magnitude, error), together with the airmass, as text files and uploaded the photometry output to the ETD to gain an initial indication of the quality of the transit (Level 1 analysis).

For more detailed analysis, we imported the text file outputs from *MuniWin* into a custom Microsoft *Excel* spreadsheet for conversion into a format suitable for use with the *EXOFAST* transit-fitting model developed by Eastman *et al.* (2013).<sup>37</sup> For this higher-fidelity analysis (Level 2), the  $V-C$  magnitudes were converted to relative fluxes and the time converted from  $JD_{UTC}$  to Barycentric Julian Date in Barycentric Dynamical Time ( $BJD_{TDB}$ ) using the online utility developed by Eastman *et al.* (2010).<sup>38</sup> For each data point, a linear de-trend parameter was calculated based on the slope of the pre- and post-transit data points as identified from the Level 1 analysis, and the fluxes normalised to an out-of-transit value of  $\sim 1$ . We then prepared an ‘output’ text file comprising:  $BJD_{TDB}$ , normalised flux, flux error, linear de-trend parameter and airmass. This file was used as the photometry input to the *EXOFAST* transit-fitting model.

A full demonstration of the use of *MuniWin* software with MicroObservatory exoplanet image data is available on YouTube.<sup>39</sup>

## Transit-fitting modelling

*EXOFAST* has become an important tool for astronomers who want to use transit light curves or radial velocity data, or both, together with various inputs, to create models of planetary systems. Originally requiring the use of the proprietary software language IDL, the NASA Exoplanet Archive has recently integrated the same IDL-based calculations as the original into its suite of web resources.<sup>3</sup> The software implements the light curve models of Mandel & Agol (2002),<sup>40</sup> as well as a differential-evolution Markov Chain Monte Carlo (MCMC) method,<sup>41,42</sup> to estimate and characterise parameters and uncertainty distributions.<sup>43</sup> The Exoplanet Archive website provides enough back-end computing resources to enable the MCMC analysis of observed transit light curves and thus relieves the user of the need to run this high-fidelity model locally.

We uploaded individual output photometry files from the *MEOW* pipeline to *EXOFAST*, and the default parameter set for HAT-P-32b required for the model was ‘pulled’ from the Exoplanet Archive. The various prior values of the required parameters, hereafter termed ‘priors’, together with their widths (uncertainties) are given in Table 2. These priors represent the default parameter values for the system in late 2016 and whilst they have been updated since then, these have been used in the analysis to maintain continuity across the observation datasets. Limb-darkening coefficients were automatically calculated by *EXOFAST* for each run. Except for the run using combined transits covering multiple epochs, a mid-transit ( $T_c$ ) prior was not specified since for transit-only fits the mean of the input times is used by the model as the prior when no midpoint is specified.

With transit-only fits, the light-curve data alone provide very little constraint on the eccentricity and longitude of periastron, both of which are required for the model. These parameters appreciably affect the derived physical parameters. Accordingly, we forced a circular orbit for the transit fits, as recommended by the *EXOFAST* documentation. Such an orbit is consistent with the near-circular solution of Zhao *et al.* (2014),<sup>29</sup> although others have derived eccentricities in the range 0.10–0.22.<sup>27,28</sup>

Since *EXOFAST* does not include a generic ‘clear’ filter for the modelling of transit light curves, we chose the *CoRoT* band as it approximates to the ‘clear’ filter used for the MicroObservatory images.<sup>44</sup>

**Table 1. Journal of observations for 43 light curves of HAT-P-32b transits**

Date (UT)	Epoch	Telescope	Observations	Airmass	Comparison stars
2013 Feb 6	215	<i>Cecilia</i>	71	1.1→2.5	C1→C8
2013 Sep 24	322	<i>Cecilia</i>	91	3.3→1.1	C1→C8
2013 Sep 26	323	<i>Cecilia</i>	97	1.3→1.0→1.1	C1→C8
2013 Oct 9	329	<i>Cecilia</i>	99	1.7→1.0	C1→C8
2013 Oct 11	330	<i>Cecilia</i>	87	1.0→1.3	C1→C8
2013 Oct 24	336	<i>Cecilia</i>	94	1.2→1.0→1.2	C1→C8
2013 Nov 6	342	<i>Cecilia</i>	97	1.5→1.0	C1→C8
2013 Nov 8	343	<i>Cecilia</i>	92	1.0→1.7	C1→C8
2013 Dec 4	355	<i>Cecilia</i>	92	1.3→1.0→1.1	C1→C8
2014 Jan 3	369	<i>Cecilia</i>	91	1.0→2.7	C1→C8
2014 Jan 16	375	<i>Cecilia</i>	91	1.0→1.7	C1→C8
2014 Oct 4	496	<i>Donald</i>	103	1.4→1.0	C1→C8
2014 Oct 18	503	<i>Cecilia</i>	99	1.1→1.0→1.3	C1→C8
2014 Oct 31	509	<i>Cecilia</i>	77	1.3→1.0→1.1	C1→C8
2014 Nov 15	516	<i>Cecilia</i>	88	1.0→1.5	C1→C8
2014 Nov 28	522	<i>Cecilia</i>	95	1.2→1.0→1.1	C1→C8
2015 Oct 23	675	<i>Cecilia</i>	86	2.4→1.0	C1→C8
2015 Nov 7	682	<i>Cecilia</i>	102	1.4→1.0	C1→C8
2015 Nov 9	683	<i>Cecilia</i>	89	1.0→1.8	C1→C8
2016 Sep 5	823	<i>Cecilia</i>	91	1.6→1.0	C1→C8
2016 Oct 3	836	<i>Cecilia</i>	89	1.6→1.0→1.1	C1→C8
2016 Oct 18	843	<i>Cecilia</i>	121	1.2→1.0→1.5	C1→C8
2016 Oct 31	849	<i>Cecilia</i>	117	1.5→1.0→1.2	C1→C8
2017 Sep 25	1002	<i>Cecilia</i>	98	3.6→1.1	C4, C9→C13
2017 Sep 27	1003	<i>Cecilia</i>	96	1.2→1.0→1.1	C1→C8
2017 Oct 10	1009	<i>Cecilia</i>	100	1.6→1.0	C1→C8
2017 Oct 23	1015	<i>Cecilia</i>	95	2.3→1.0	C1→C8
2017 Nov 7	1022	<i>Cecilia</i>	95	1.5→1.0→1.1	C2→C4
2017 Nov 22	1029	<i>Cecilia</i>	104	1.1→1.0→1.4	C1→C8
2017 Dec 20	1042	<i>Cecilia</i>	122	1.1→1.0→1.7	C1→C8
2018 Nov 1	1189	<i>Cecilia</i>	101	1.2→1.0→1.1	C1→C8
2018 Nov 14	1195	<i>Cecilia</i>	95	1.7→1.0	C1→C8
2018 Nov 29	1202	<i>Cecilia</i>	90	1.2→1.0→1.1	C1→C8
2018 Dec 14	1209	<i>Cecilia</i>	93	1.0→1.6	C1→C8
2019 Jan 11	1222	<i>Cecilia</i>	92	1.0→2.2	C1→C8
2019 Sep 13	1336	<i>Cecilia</i>	91	1.8→1.0	C1→C4
2019 Sep 28	1343	<i>Cecilia</i>	104	1.2→1.0→1.1	C1
2019 Oct 24	1355	<i>Cecilia</i>	102	2.5→1.0	C1→C4
2019 Dec 6	1375	<i>Cecilia</i>	103	1.3→1.0→1.1	C1→C4
2019 Dec 21	1382	<i>Cecilia</i>	102	1.0→1.5	C1
2020 Jan 5	1389	<i>Cecilia</i>	100	1.0→3.0	C1→C4
2020 Jan 18	1395	<i>Cecilia</i>	103	1.0→1.8	C1→C4
2020 Feb 2	1402	<i>Cecilia</i>	85	1.1→4.2	C1→C4

**Table 2. HAT-P-32b prior value & width inputs for *EXOFAST* modelling**

Prior parameter	Prior value	Prior width
Orbital inclination, $i$ (degrees)	88.9	–
Stellar effective temp., $T_{eff}$ (Kelvin)	6269	64.0
Metallicity, [Fe/H] (dex)	–0.04	0.08
Orbital period, $P$ (d)	2.15000805	0.00000095
Eccentricity, $e$	0.0	–
Longitude of periastron, $\omega^*$ (degrees)	90.0	–

MCMC fits were successfully run on 28 of the 43 transit light curves. The failures of the remaining 15 light curves were mainly because of the presence of NaN (‘not a number’) errors, which caused the *EXOFAST\_PLOTDIST* routine to halt and no output to be produced. Unfortunately, this could not be addressed because of the reduced input parameters of the flavour of *EXOFAST* run on the Exoplanet Archive website compared with the full offline version. For these transits, chi-squared ( $\chi^2$ ) fits were successfully made using the model, although it should be noted that the uncertainties of the derived parameters from these fits are analytical approximations rather than the more accurate statistical estimations determined by the MCMC fits.<sup>45</sup>

## Analysis of transit light curves

A representative model fit (with residuals) to the observed light curve of the HAT-P-32b transit observed on 2019 Dec 6 (epoch 1375) is shown in Figure 2. All 43 light curves, together with their respective modelled transit curves, are shown in Figure 3. The light curves show well-defined transits, albeit with varying degrees of scatter around the transit curves. Key derived parameters, including median times of mid-transit ( $T_C$ ), total duration (1st to 4th contact,  $T_{14}$ ) and transit depth, are tabulated for each transit in Table 3.

### Mid-transit times

Wang *et al.* (2019) have recently refined the linear ephemeris of the HAT-P-32b system to be:<sup>28</sup>

$$T_C(N) = 2455867.402743 (49) + N \cdot 2.15000820 (13)$$

where  $N$  represents the number of orbital cycles (epochs) since the reference epoch (given in  $\text{BJD}_{\text{TDB}}$ ) and the bracketed

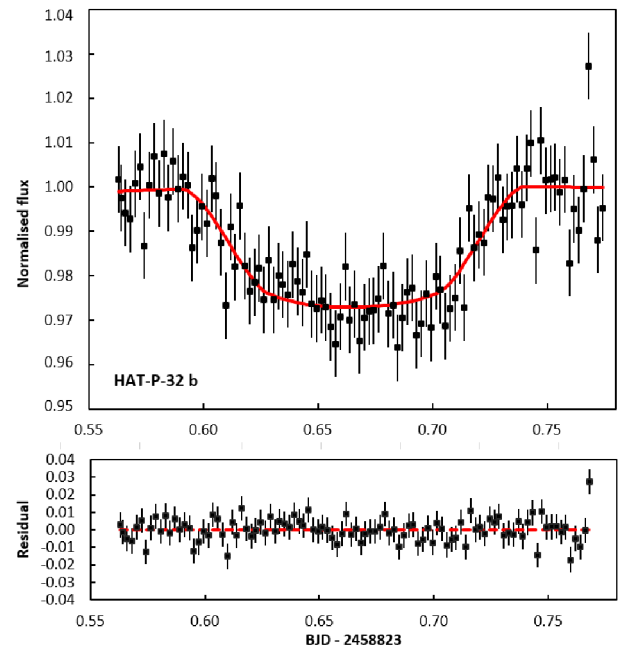


**Figure 2.** Representative transit light curve of HAT-P-32b for observations of 2019 Dec 6 (epoch 1375), together with the modelled transit fit using *EXOFAST*.

**Table 3. Derived parameters & 68% confidence intervals for 43 transits of HAT-P-32b**

Date (UT)	Epoch	Fit type	RMS residuals	Time of mid-transit, $T_C$ ( $\text{BJD}_{\text{TDB}}$ )	O-C (min)	Total duration, $T_{14}$ (min)	Depth (%)
2013 Feb 6	215	Chi2	0.007	2456329.6556 ±0.0019	1.5	195.6 ±10.8	2.2 ±0.1
2013 Sep 24	322	Chi2	0.010	2456559.7043 ±0.0017	-1.5	180.6 ±9.6	3.0 ±0.2
2013 Sep 26	323	MCMC	0.007	2456561.8566 ±0.0026	1.8	193.1 ±17.9	2.5 ±0.6
2013 Oct 9	329	MCMC	0.007	2456574.7597 ±0.0024	6.1	213.9 ±24.8	2.9 ±0.8
2013 Oct 11	330	MCMC	0.007	2456576.9060 ±0.0019	0.8	200.3 ±9.9	3.0 ±0.8
2013 Oct 24	336	Chi2	0.008	2456589.8052 ±0.0017	-0.4	186.7 ±9.8	2.1 ±0.1
2013 Nov 6	342	Chi2	0.008	2456602.7079 ±0.0017	3.3	180.4 ±9.7	2.8 ±0.1
2013 Nov 8	343	MCMC	0.007	2456604.8559 ±0.0014	0.5	188.6 ±6.0	2.6 ±0.3
2013 Dec 4	355	Chi2	0.008	2456630.6559 ±0.0021	0.4	216.8 ±12.0	2.5 ±0.1
2014 Jan 3	369	Chi2	0.007	2456660.7537 ±0.0013	-2.9	190.2 ±16.1	2.4 ±0.1
2014 Jan 16	375	Chi2	0.010	2456673.6560 ±0.0022	0.2	178.4 ±12.4	2.2 ±0.2
2014 Oct 4	496	MCMC	0.004	2456933.8061 ±0.0009	-1.1	191.4 ±6.1	2.6 ±0.2
2014 Oct 18	503	MCMC	0.005	2456948.8583 ±0.0022	2.1	203.1 ±31.9	2.8 ±1.0
2014 Oct 31	509	MCMC	0.005	2456961.7574 ±0.0024	0.7	193.3 ±34.2	2.3 ±71.4
2014 Nov 15	516	MCMC	0.006	2456976.8059 ±0.0023	-1.5	194.7 ±33.1	2.5 ±16.4
2014 Nov 28	522	MCMC	0.005	2456989.7067 ±0.0012	-0.4	210.2 ±11.3	3.1 ±0.4
2015 Oct 23	675	MCMC	0.006	2457318.6592 ±0.0013	1.3	199.6 ±8.0	2.9 ±0.4
2015 Nov 7	682	MCMC	0.006	2457333.7105 ±0.0022	3.2	162.8 ±8.5	2.2 ±0.9
2015 Nov 9	683	MCMC	0.006	2457335.8567 ±0.0025	-2.3	193.8 ±25.3	2.4 ±0.6
2016 Sep 5	823	MCMC	0.007	2457636.8569 ±0.0018	-3.7	215.1 ±13.7	2.7 ±0.6
2016 Oct 3	836	MCMC	0.007	2457664.8105 ±0.0021	1.4	193.4 ±11.2	2.1 ±0.3
2016 Oct 18	843	MCMC	0.007	2457679.8601 ±0.0016	0.6	192.2 ±11.4	2.8 ±0.3
2016 Oct 31	849	MCMC	0.007	2457692.7620 ±0.0017	3.3	198.9 ±9.2	2.9 ±0.3
2017 Sep 25	1002	Chi2	0.009	2458021.7084 ±0.0022	-3.7	186.6 ±12.4	1.9 ±0.1
2017 Sep 27	1003	MCMC	0.005	2458023.8619 ±0.0012	1.4	188.0 ±9.2	2.8 ±0.3
2017 Oct 10	1009	MCMC	0.005	2458036.7623 ±0.0012	1.9	195.1 ±9.8	2.4 ±0.3
2017 Oct 23	1015	Chi2	0.007	2458049.6618 ±0.0011	1.1	188.8 ±6.6	2.5 ±0.1
2017 Nov 7	1022	MCMC	0.008	2458064.7114 ±0.0025	0.4	198.3 ±18.0	2.4 ±0.4
2017 Nov 22	1029	MCMC	0.006	2458079.7598 ±0.0019	-2.0	192.2 ±13.0	2.5 ±0.3
2017 Dec 20	1042	MCMC	0.006	2458107.7118 ±0.0014	0.7	176.2 ±6.1	2.2 ±0.2
2018 Nov 1	1189	MCMC	0.007	2458423.7592 ±0.0015	-4.7	185.9 ±5.7	2.0 ±0.2
2018 Nov 14	1195	Chi2	0.013	2458436.6638 ±0.0022	1.7	196.8 ±12.5	2.9 ±0.2
2018 Nov 29	1202	MCMC	0.007	2458451.7056 ±0.0016	-10.1	174.3 ±7.3	2.0 ±0.2
2018 Dec 14	1209	Chi2	0.010	2458466.7637 ±0.0025	1.5	179.5 ±14.3	1.8 ±0.2
2019 Jan 11	1222	MCMC	0.009	2458494.7074 ±0.0018	-7.8	187.5 ±11.7	2.4 ±0.3
2019 Sep 13	1336	Chi2	0.008	2458739.8133 ±0.0003	-0.5	207.8 ±17.1	1.4 ±0.1
2019 Sep 28	1343	MCMC	0.007	2458754.8637 ±0.0026	-0.1	195.3 ±5.6	3.9 ±3.9
2019 Oct 24	1355	MCMC	0.007	2458780.6648 ±0.0002	1.4	186.9 ±11.1	1.7 ±0.2
2019 Dec 6	1375	MCMC	0.007	2458823.6659 ±0.0025	2.8	216.3 ±30.9	2.6 ±16.7
2019 Dec 21	1382	MCMC	0.011	2458838.7139 ±0.0017	-0.3	172.9 ±16.6	2.2 ±0.5
2020 Jan 5	1389	Chi2	0.011	2458853.7616 ±0.0026	-3.7	181.1 ±15.2	1.9 ±0.2
2020 Jan 18	1395	MCMC	0.008	2458866.6615 ±0.0021	-3.9	187.9 ±12.3	2.3 ±0.3
2020 Feb 2	1402	Chi2	0.011	2458881.7117 ±0.0027	-3.7	184.2 ±15.3	2.0 ±0.2

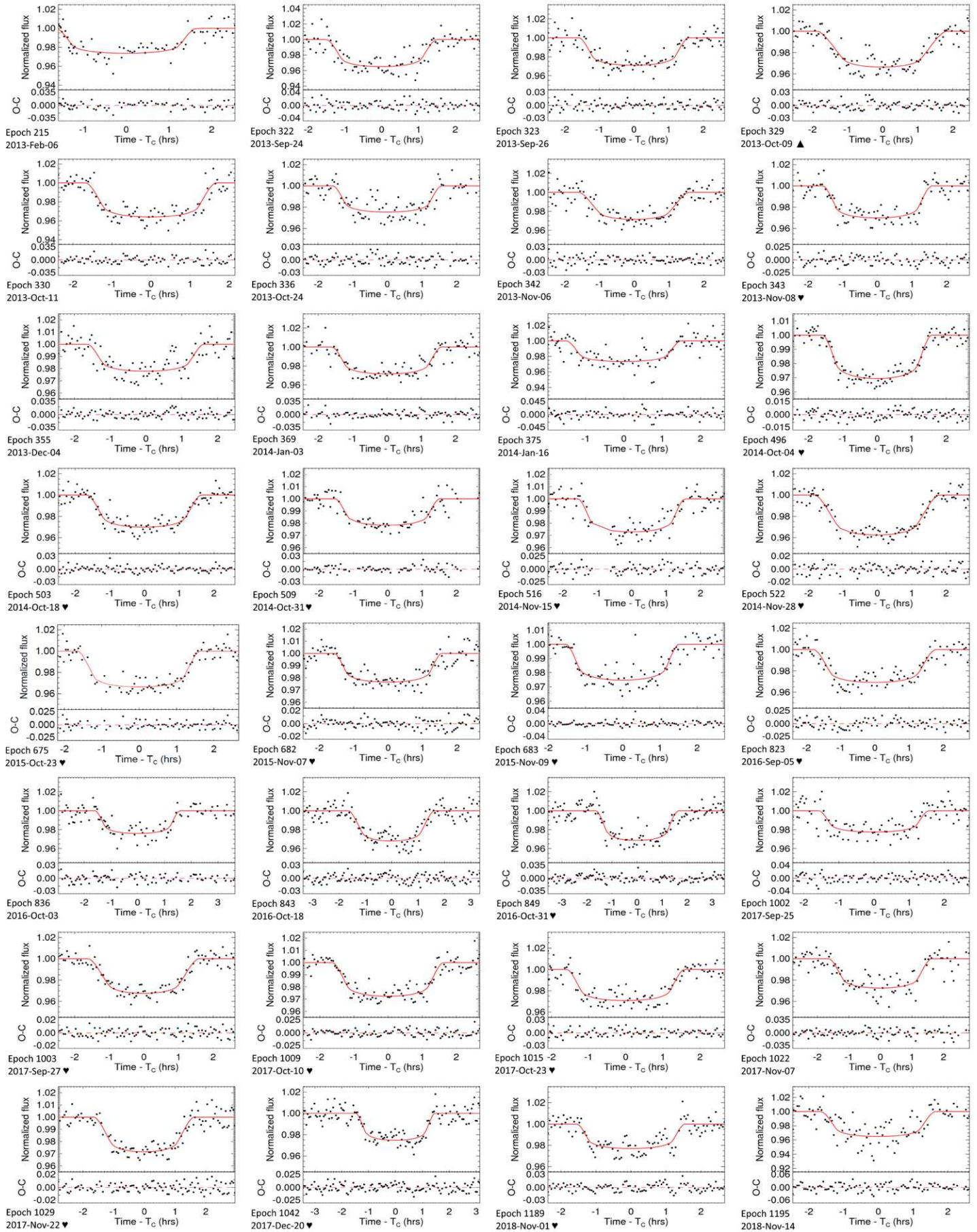


**Figure 3.** Transit light curves and *EXOFAST* model fits for 43 transits of HAT-P-32b observed by MicroObservatory (figure continued next page). The three transits exhibiting  $T_c$   $O-C$  values in excess of  $\pm 6$ min are annotated with a triangle ( $\blacktriangle$ ) after the transit date. Likewise, the top 20 transits used to determine the HAT-P-32b system parameters are annotated with a heart ( $\heartsuit$ ).

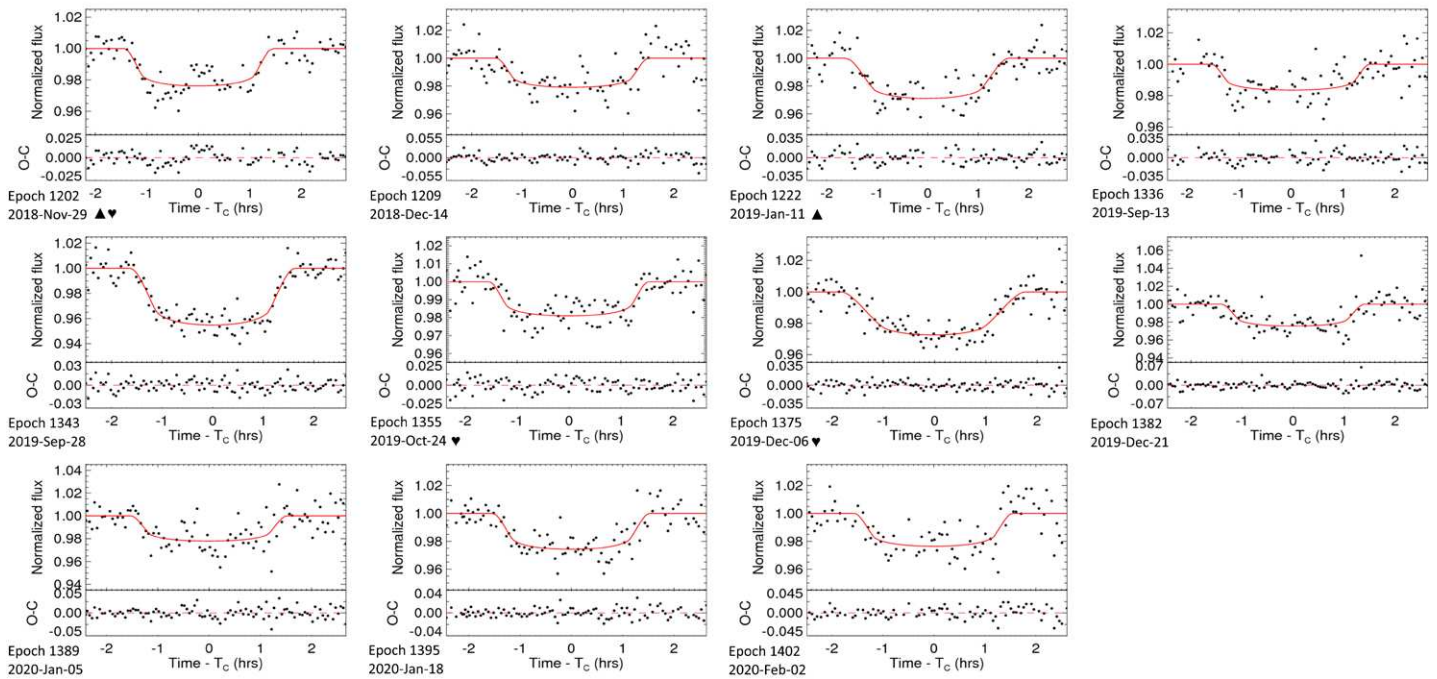


Figure 3 (Continued). See caption on p.363.

quantities represent the uncertainty in the final two digits of the preceding number.

A plot of the observed-minus-calculated ( $O-C$ ) values for  $T_C$  based on this ephemeris is shown in Figure 4. The mean of  $O-C$  values is  $-0.3 \pm 3.0$ min and the scatter of all the mid-transit times has a root mean square (RMS) of 3.0min. The reduced chi-squared statistic ( $\chi^2_\nu$ ) is 1.02 with 42 degrees of freedom, indicating that the observed mid-transit times agree with the calculated times at the one-sigma level.

Three of the transits have  $T_C$   $O-C$  values that are in excess of  $\pm 6$ min. The transit of 2013 Oct 9 (epoch 329) has a  $T_C$  that is 6.1min late, whereas the transits of 2018 Nov 29 (epoch 1202) and 2019 Jan 11 (epoch 1222) are respectively 10.1 and 7.8min early. Whilst these *could* reflect TTVs due to another unknown body in the system, the transit light curves for these sets of observations are relatively noisy (as highlighted in Figure 3) and in the latter two cases the transits are somewhat poorly defined, suggesting that they are likely to be artefacts rather than actual TTVs.

### Transit duration

A histogram of the total transit durations (1st to 4th contact,  $T_{14}$ ) of the 43 observed transits is shown in Figure 5. The weighted mean transit duration is  $189.1 \pm 12$ min and this compares well with the estimate of Wang *et al.* of  $187.2 \pm 0.8$ , although the error of the MicroObservatory observations is over an order of magnitude greater and reflects the greater noise of the transit observations.

### Transit depth

Likewise, a histogram of the transit depth of the 43 observed transits is shown in Figure 6. The weighted mean transit depth is  $2.28 \pm 0.45\%$  and is comparable to the depth of  $2.216 \pm 0.017\%$

reported by Wang *et al.*, who used a red filter for their observations rather than unfiltered observations as used in this study.

## Estimating the HAT-P-32b system parameters

We estimated the HAT-P-32b system parameters from the current observations by running the combined photometry from the top 20 transits, as determined by their individual RMS residuals, in *EXOFAST*. Priors and widths were as before except that in this case a  $T_C$  prior of  $2457692.7597 \pm 0.0020$ BJD<sub>TDB</sub> was used, as this equates to the predicted  $T_C$  for the median transit of the set (2016 Oct 31, epoch 849), based on the Wang *et al.* ephemeris given above.

The resulting combined transit light curve of the 1,952 data points is shown in Figure 7, with the median values and 68% confidence intervals for the system parameters given in Table 4 (p.367). As can be seen, the estimated system parameters are broadly consistent with those of Wang *et al.*, which were the default parameter values listed in the NASA Exoplanet Archive for the HAT-P-32b system at the time of writing.

## Calculating an updated ephemeris

Using the derived mid-transit times and uncertainties for our 43 observed transits of HAT-P-32b, we can calculate an updated ephemeris to predict future transit events more accurately. To illustrate the power of follow-up observations to refine the original ephemeris, we use the original discovery ephemeris of Hartman *et al.* (2011) as priors for the system,<sup>27</sup> and solve for HAT-P-32b's orbital period and ephemeris with a MCMC fit to our MicroObservatory results,<sup>41</sup> following the procedure explained, for example, in detail by Zellem *et al.* (2020).<sup>18</sup> From this we find an

orbital period of  $2.15000711 \pm 0.00000057\text{d}$  and ephemeris of  $2458881.71327 \pm 0.00044\text{BJD}_{\text{TDB}}$ . Likewise, to illustrate the value of follow-up observations even with existing high-precision data, we use the default parameter values in the NASA Exoplanet Archive (*i.e.*, Wang *et al.*<sup>28</sup>) as priors to the MCMC fit, to find an orbital period of  $2.15000815 \pm 0.00000013\text{d}$  and ephemeris of  $2458881.71392 \pm 0.00027\text{BJD}_{\text{TDB}}$ .

Taking these updated ephemerides and propagating the errors forward as described in Zellem *et al.*,<sup>18</sup> we can estimate the  $T_C$  for a NASA JWST mission in mid-2021. When we use the discovery ephemeris as priors to the MCMC fit, we calculate the  $T_C$  of a notional transit of HAT-P-32b on 2021 May 30 to be like that using the discovery ephemeris alone (Figure 8A). However, it is  $\sim 4$  times more precise and thus shows the benefit of the follow-up observations to refine the precision of the original ephemeris. When we use the NASA Exoplanet Archive ephemeris as the priors to the MCMC fit, the calculated  $T_C$  is 1.4min later and  $\sim 8$  times more precise than that calculated using the discovery ephemeris, which at that time would be over 13 years old. Indeed, this estimate is only slightly less accurate and 0.5min earlier than that calculated using the ephemeris given in the NASA Exoplanet Archive and shows the value of follow-up observations, even with existing high-precision data.

In the case of an ESA ARIEL mission in 2028, we find that the shorter orbital period determined by the MCMC fit using the discovery ephemeris as priors gives an estimated  $T_C$  that is 1.3min earlier than that using the discovery ephemeris alone. However, when we use the MCMC fit with the NASA Exoplanet Archive ephemeris as the prior, we find a  $T_C$  that is consistent with that obtained using the NASA Exoplanet Archive and 1.7min later than that predicted using the discovery ephemeris (Figure 8B).

On this basis, we propose an updated ephemeris of the HAT-P-32b system of:

$$T_C(N) = 2458881.71392 (27) + N \cdot 2.15000815 (13)$$

where, again, the bracketed quantities represent the uncertainty in the final two digits of the preceding number. Whilst there is a

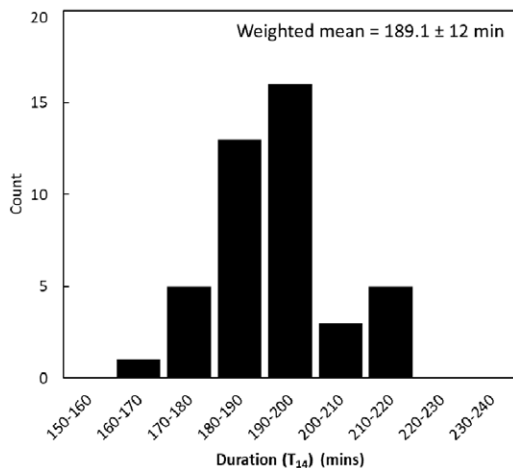


Figure 5. Distribution of transit durations (1st to 4th contact,  $T_{14}$ ) for the 43 observed transits of HAT-P-32b.

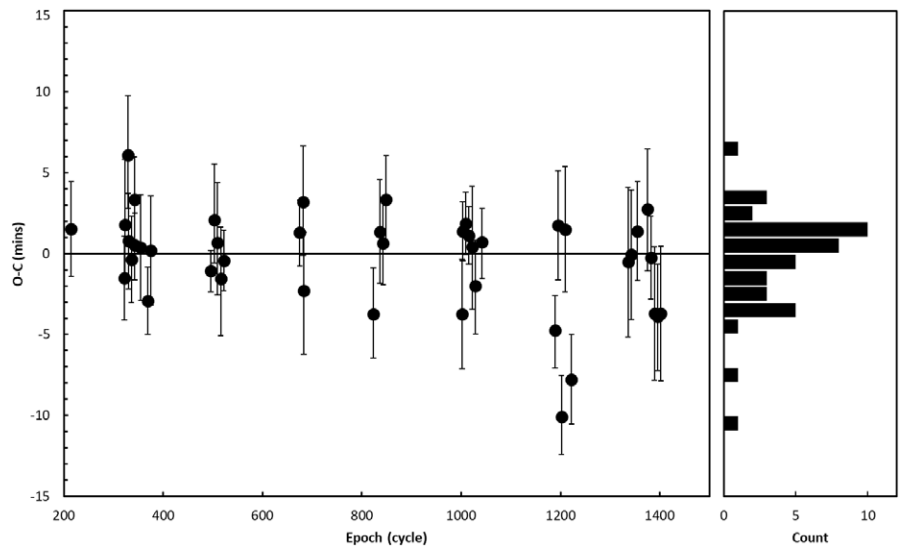


Figure 4. Observed-minus-calculated ( $O-C$ ) mid-transit ( $T_C$ ) residuals for the 43 observed transits of HAT-P-32b, together with a histogram showing the distribution of the individual values. The  $T_C$  residuals were calculated using the ephemeris of Wang *et al.* (2019).

small difference in the period compared with that determined using the *EXOFAST* analysis of the top 20 transit curves (see Table 4), it is nevertheless contained within the larger uncertainty of the *EXOFAST* estimate.

## Discussion & conclusions

In this work we have presented 43 complete transit light curves of the hot Jupiter HAT-P-32b, acquired by the MicroObservatory robotic telescope network. Compared with the most recent estimate of the ephemeris of the system by Wang *et al.*,<sup>28</sup> the mean of the  $T_C$   $O-C$  values is  $-0.3 \pm 3.0\text{min}$  and the scatter of all the mid-transit times has an RMS of 3.0min, which is similar to the nominal cadence of the observations. Although three of the transits show  $T_C$   $O-C$  values that are greater than  $\pm 6\text{min}$ , the transit light curves are quite noisy, with two of the transits being somewhat poorly defined. Since Seeliger *et al.* have shown that transit timing analysis of the HAT-P-32 system excludes TTVs of more than  $\sim 1.5\text{min}$ ,<sup>34</sup> these outlier points on the  $O-C$  plot are considered to be artefacts rather than actual TTVs.

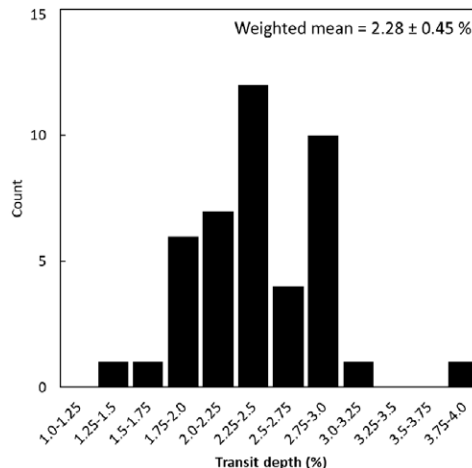
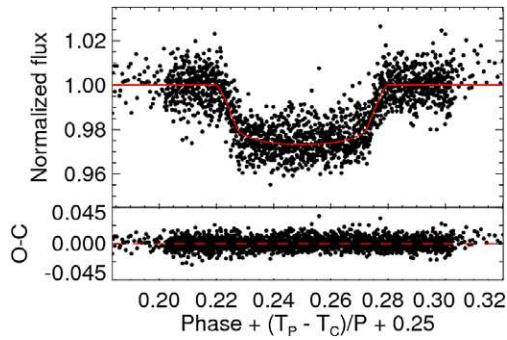


Figure 6. Distribution of transit depths for the 43 observed transits of HAT-P-32b.

The mean total transit duration ( $T_{14}$ ) and transit depth are comparable with the Wang *et al.* estimates. Similarly, the estimated system parameters based on *EXOFAST* modelling of the combined top 20 transit light curves are broadly consistent with those of Wang *et al.* These represent the default parameter values listed in the NASA Exoplanet Archive and indicate that observations using MicroObservatory can be used to characterise exoplanet systems to a reasonable degree of accuracy.

As noted above, observations of transiting exoplanets by amateurs,



**Figure 7.** Combined transit light curve and *EXOFAST*-modelled transit based on the observations of 20 transits of HAT-P-32b. The x-axis is essentially the phase offset, so that the mid-transit occurs at 0.25.

and other users of small ( $\leq 1\text{m}$ ) telescopes, can contribute to the maintenance of the ephemerides of targets for future space-based telescope missions that will investigate exoplanets.<sup>17,18</sup> Our updated ephemeris improves the predicted  $T_C$  for an observation of HAT-P-32b by a JWST mission in mid-2021 by 1.4min compared with the discovery ephemeris and is  $\sim 8$  times more precise. The prediction is slightly less accurate and 0.5min earlier than that calculated using the ephemeris in the NASA Exoplanet Archive. Likewise, when we use our updated ephemeris for an observation of HAT-P-32b by the ARIEL mission in 2028, we find a  $T_C$  that is 1.7min later than that predicted using the discovery ephemeris and consistent with that obtained using the NASA Exoplanet Archive alone. Thus, our HAT-P-32b observations can be seen to significantly improve the original ephemeris of the system to a level consistent with recent studies using larger telescopes. Furthermore, we anticipate that observations using MicroObservatory and other small telescopes could be used to substantially refine the ephemerides of targets with larger uncertainties.

The current 30 exoplanet targets that are routinely observed by MicroObservatory throughout the year have V-band magnitudes in the range 10.3 to 14.1 and depths of transit between 1.5 and 2.9%. For 2019, we find the annual utilisation of the MicroObservatory telescope *Cecilia* in observing these targets was  $\sim 77\%$ . Since the telescope is dedicated to observing exoplanet transits, the spare observing capacity, equivalent to  $\sim 84$  nights of observations per year, could be directed towards the observation of new targets that are within the capabilities of the telescope, including some of those identified as being ideal for TTV measurements by small ground-based observatories.<sup>18</sup>

With a field of view of approximately  $0.72\text{deg}^2$  the HAT-P-32 images show over 400 discrete stars, including the 13.9 V-magnitude  $\delta$  Scuti variable star UCAC4 686-012519 (= ASASSN-V J020549.64+470040.9), which has been further characterised using the same observations as our study.<sup>46</sup> This finding demonstrates the potential for MicroObservatory to observe stellar variability, whilst simultaneously observing transiting exoplanets for ephemeris maintenance.<sup>18</sup>

## Acknowledgements

We thank Jason Eastman for his advice on running *EXOFAST* and for commenting on an early version of this paper. The paper makes use of *EXOFAST* (Eastman et al., 2013) as provided by the

NASA Exoplanet Archive, which is operated by the California Institute of Technology, under contract with the National Aeronautics and Space Administration under the Exoplanet Exploration Program.

MicroObservatory is maintained and operated as an educational service by the Center for Astrophysics, Harvard & Smithsonian and is a project of NASA’s Universe of Learning, supported by NASA award no. NNX16AC65A. Additional MicroObservatory sponsors include the National Science Foundation, NASA, the Arthur Vining Davis Foundations, Harvard University and the Smithsonian Institution. This research has made use of NASA’s Astrophysical Data System (ADS) and the NASA Exoplanet Archive. The paper makes use of data tools and/or products from Exoplanet Watch, a citizen science project managed by NASA’s Jet Propulsion Laboratory on behalf of NASA’s Universe of Learning. This work is supported by NASA under award no. NNX16AC65A to the Space Telescope Science Institute.

Part of the research was carried out at the Jet Propulsion Laboratory, California Institute of Technology, under contract with the National Aeronautics and Space Administration. We thank Richard Miles and Roger Dymock for helpful comments that have improved the paper.

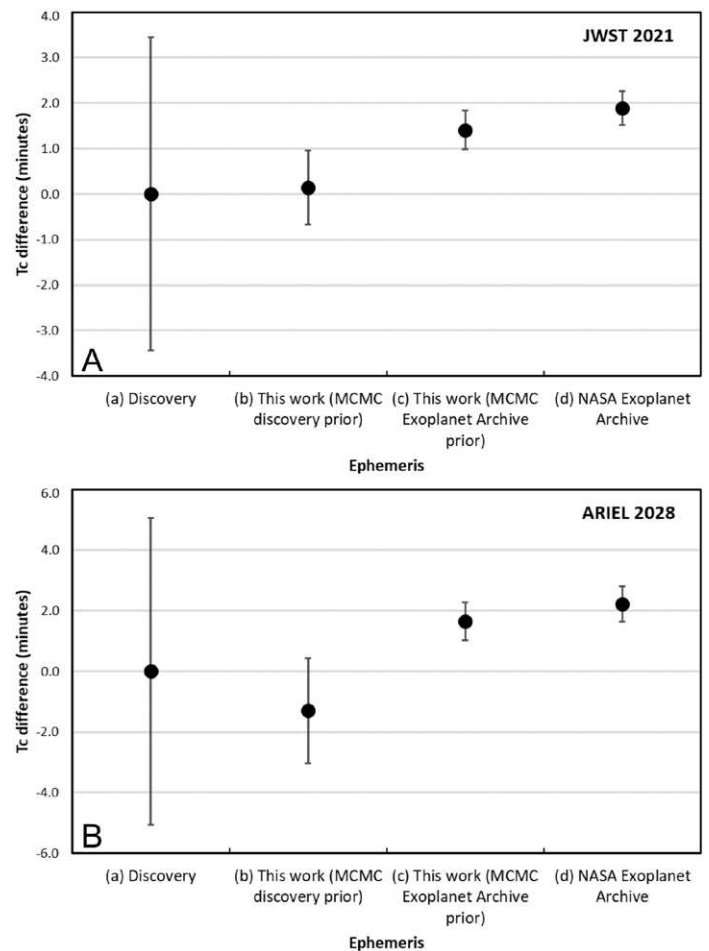


**Figure 8.** Comparison of estimated mid-transit times ( $T_C$ ) for the observation of a notional HAT-P-32b transit by (A) the NASA JWST mission in mid-2021 and (B) the ESA ARIEL mission in 2028. Different ephemerides are used to estimate  $T_C$ : (a) the original discovery ephemeris; (b) an MCMC fit to the observations reported in this work using the discovery ephemeris as the prior; (c) a similar MCMC fit but using the NASA Exoplanet Archive ephemeris as the prior; (d) the NASA Exoplanet Archive ephemeris. The differences in  $T_C$  are shown relative to the  $T_C$  value estimated using the discovery ephemeris (i.e.,  $2459365.464770 \pm 0.00239\text{BJD}_{\text{TDB}}$  for the JWST and  $2461771.323722 \pm 0.00351\text{BJD}_{\text{TDB}}$  for ARIEL).

## Addresses

**MJFF:** Les Rocquettes, Orchard Road, South Wonston, Winchester, SO21 3EX, UK [danebury216@hotmail.co.uk]. **FFS** and **MED:** Science Education Department, The Center for Astrophysics | Harvard & Smithsonian, 60 Garden Street, Cambridge, Massachusetts, 02138, USA [fsienkiewicz@cfa.harvard.edu;mdussault@cfa.harvard.edu]. **RTZ:** Jet Propulsion Laboratory, California Institute of Technology, 4800 Oak Grove Drive, Pasadena, California, 91109, USA [robert.t.zellem@jpl.nasa.gov].

## References &amp; notes

- 1 Mayor M. & Queloz D., ‘A Jupiter-mass companion to a solar-type star’, *Nature*, **378**, 355–359 (1995)
- 2 Akeson R. L. *et al.*, ‘The NASA Exoplanet Archive: data and tools for exoplanet research’, *Publ. Astron. Soc. Pacific*, **125**, 989–999 (2013)
- 3 NASA Exoplanet Archive (2020). Available at: <https://exoplanetarchive.ipac.caltech.edu/index.html> (accessed 2020 April).
- 4 Spiegel D. S., Fortney J. J. & Sotin C., ‘Structure of exoplanets’, *Proc. Natl. Acad. Sci.*, **111**, 12622–12627 (2014)
- 5 Winn J. N. & Fabrycky D. C., ‘The occurrence and architecture of exoplanetary systems’, *Annu. Rev. Astron. Astrophys.*, **53**, 409–447 (2014)
- 6 Haswell C. A., *Transiting exoplanets*, Cambridge University Press, 2010
- 7 Bakos G. Á., ‘The HATNet and HATSouth exoplanet surveys’, *arXiv Prepr.*, **1801.00849**, 1–11 (2018)
- 8 Pollacco D. L. *et al.*, ‘The WASP Project and the SuperWASP cameras’, *Publ. Astron. Soc. Pacific*, **118**, 1407–1418 (2006)
- 9 Perryman M., *The exoplanet handbook*, 2nd edn, Cambridge University Press, 2018
- 10 Lissauer J. J., Dawson R. I. & Tremaine S., ‘Advances in exoplanet science from *Kepler*’, *Nature*, **513**, 336–344 (2014)
- 11 Barclay T., Pepper J. & Quintana E. V., ‘A revised exoplanet yield from the *Transiting Exoplanet Survey Satellite* (TESS)’, *Astrophys. J. Suppl. Ser.*, **239**(2), 15pp (2018)
- 12 Sergison D., ‘High precision photometry: detection of exoplanet transits using a small telescope’, *J. Brit. Astron. Assoc.*, **123**, 153–156 (2013)
- 13 Poddaný S., Brát L. & Pejcha O., ‘Exoplanet Transit Database. Reduction and processing of the photometric data of exoplanet transits’, *New Astron.*, **15**, 297–301 (2010)
- 14 Baluev R. V. *et al.*, ‘Benchmarking the power of amateur observatories for TTV exoplanets detection’, *Mon. Not. R. Astron. Soc.*, **450**, 3101–3113 (2015)
- 15 Baluev R. V. *et al.*, ‘Homogeneously derived transit timings for 17 exoplanets and reassessed TTV trends for WASP-12 and WASP-4’, *Mon. Not. R. Astron. Soc.*, **490**, 1294–1312 (2019)
- 16 Mallonn M. *et al.*, ‘Ephemeris refinement of 21 hot Jupiter exoplanets with high timing uncertainties’, *Astron. Astrophys.*, **622**, A81 (2019)
- 17 Zellem R. T. *et al.*, ‘Engaging citizen scientists to keep transit times fresh and ensure the efficient use of transiting exoplanet characterization missions’, *arXiv Prepr.*, **1903.07716**, 1–6 (2019)
- 18 Zellem R. T. *et al.*, ‘Utilizing small telescopes operated by citizen scientists for transiting exoplanet follow-up’, *Publ. Astron. Soc. Pacific*, **132**, 054401 (2020)
- 19 NASA Exoplanet Watch. Available at: <https://exoplanets.nasa.gov/exoplanet-watch/> (accessed 2020 April).
- 20 Kokori A. & Tsiaras A., ‘ExoWorlds Spies: a project for public involvement in exoplanet research’, *EPSC Abstr.*, **12**, EPSC2018-1268-1 (2018)
- 21 ARIEL ExoClock Project, by the ARIEL Ephemerides Working Group. Available at: <https://www.exoclock.space/> (accessed 2020 April).
- 22 Gould R. R., Sunbury S. & Krumhansl R., ‘Using online telescopes to explore exoplanets from the physics classroom’, *Am. J. Phys.*, **80**, 445–451 (2012)
- 23 Gould R., Sunbury S. & Dussault M., ‘In praise of messy data: Lessons from the search for alien worlds’, *Sci. Teach.*, 31–37 (2014)
- 24 NASA’s Universe of Learning. Available at: <https://www.universe-of-learning.org/> (accessed 2020 April).
- 25 DIY Planet Search. Available at: <https://www.cfa.harvard.edu/smgph/otherworlds/OE/> (accessed 2020 April).

- 26 Fowler M. J. F., ‘Observing transiting ‘hot Jupiter’ exoplanets with the MicroObservatory’, *J. Br. Astron. Assoc.*, **129**, 174–175 (2019)
- 27 Hartman J. D. *et al.*, ‘HAT-P-32b and HAT-P-33b: Two highly inflated hot Jupiters transiting high-jitter stars’, *Astrophys. J.*, **742**, 59 (2011)
- 28 Wang Y.-H. *et al.*, ‘Transiting Exoplanet Monitoring Project (TEMP). V. Transit follow up for HAT-P-9b, HAT-P-32b, and HAT-P-36b’, *Astron. J.*, **157**, 82 (2019)

**Table 4. Median values & 68% confidence intervals for HAT-P-32b system parameters**

Parameter	Definition & units	This work	Wang <i>et al.</i> (2019)
<b>Stellar parameters:</b>			
$M_*$	Mass ( $M_\odot$ )	1.196 <sup>+0.061</sup> <sub>−0.056</sub>	1.132 <sup>+0.051</sup> <sub>−0.050</sub>
$R_*$	Radius ( $R_\odot$ )	1.228 <sup>+0.032</sup> <sub>−0.027</sub>	1.367 <sup>+0.031</sup> <sub>−0.030</sub>
$L_*$	Luminosity ( $L_\odot$ )	2.10 <sup>+0.15</sup> <sub>−0.13</sub>	2.178 <sup>+0.099</sup> <sub>−0.096</sub>
$\rho_*$	Density (cgs)	0.917 <sup>+0.034</sup> <sub>−0.052</sub>	0.625 <sup>±0.014</sup>
$\text{Log}(g_*)$	Surface gravity (cgs)	4.338 <sup>+0.013</sup> <sub>−0.017</sub>	4.22 <sup>±0.04</sup>
$T_{\text{eff}}$	Effective temperature (K)	6274 <sup>±64</sup>	6001 <sup>±88</sup>
[Fe/H]	Metallicity (dex)	−0.44 <sup>+0.078</sup> <sub>−0.080</sub>	−0.16 <sup>±0.08</sup>
<b>Planetary parameters:</b>			
$P$	Period (d)	2.15000796 <sup>±0.00000069</sup>	2.15000820 <sup>±0.00000013</sup>
$a$	Semi-major axis (au)	0.0346 <sup>+0.00058</sup> <sub>−0.00054</sub>	0.03397 <sup>+0.00051</sup> <sub>−0.00050</sub>
$R_p$	Radius ( $R_J$ )	1.810 <sup>+0.053</sup> <sub>−0.042</sub>	1.980 <sup>±0.045</sup>
$T_{\text{eq}}$	Equilibrium temp. (K)	1802 <sup>+24</sup> <sub>−22</sub>	1835.7 <sup>+6.8</sup> <sub>−6.9</sub>
$\langle F \rangle$	Incident flux ( $10^9 \text{erg s}^{-1} \text{cm}^{-2}$ )	2.39 <sup>+0.13</sup> <sub>−0.11</sub>	2.505 <sup>+0.042</sup> <sub>−0.052</sub>
<b>Primary transit parameters</b>			
$T_C$	Time of transit (BJD <sub>TDB</sub> )	2457692.75939 <sup>+0.00031</sup> <sub>−0.00030</sub>	2455867.402743 <sup>±0.000049</sup>
$R_p/R_*$	Radius of planet in stellar radii	0.1517 <sup>±0.0015</sup>	0.14886 <sup>+0.00056</sup> <sub>−0.00054</sub>
$a/R_*$	Semi-major axis in stellar radii	6.071 <sup>+0.073</sup> <sub>−0.12</sub>	5.344 <sup>+0.040</sup> <sub>−0.039</sub>
$u_1$	Linear limb-darkening coeff.	0.287 <sup>+0.042</sup> <sub>−0.041</sub>	0.316 ...
$u_2$	Quadratic limb-darkening coeff.	0.283 <sup>+0.048</sup> <sub>−0.047</sub>	0.303 ...
$i$	Inclination (degrees)	88.8 <sup>+0.83</sup> <sub>−1.1</sub>	88.98 <sup>+0.68</sup> <sub>−0.85</sub>
$b$	Impact parameter	0.128 <sup>+0.11</sup> <sub>−0.09</sub>	0.083 <sup>+0.070</sup> <sub>−0.055</sub>
$\delta$	Transit depth	0.023 <sup>±0.0004</sup>	0.02216 <sup>+0.00017</sup> <sub>−0.00016</sub>
$T_{\text{FWHM}}$	FWHM duration (d)	0.11202 <sup>+0.00097</sup> <sub>−0.00090</sub>	0.11284 <sup>+0.00037</sup> <sub>−0.00038</sub>
$\tau$	Ingress/egress duration (d)	0.01745 <sup>+0.00085</sup> <sub>−0.00033</sub>	0.01712 <sup>+0.00032</sup> <sub>−0.00015</sub>
$T_{14}$	Total duration (d)	0.1297 <sup>+0.0012</sup> <sub>−0.0011</sub>	0.13002 <sup>+0.00052</sup> <sub>−0.00049</sub>
$F_0$	Baseline flux	0.99873 <sup>+0.00024</sup> <sub>−0.00025</sub>	0.99940 <sup>±0.00013</sup>
<b>Secondary eclipse parameters:</b>			
$T_S$	Time of eclipse (BJD <sub>TDB</sub> )	2457693.83440 <sup>+0.00031</sup> <sub>−0.00030</sub>	2456236.268 <sup>+0.10</sup> <sub>−0.098</sub>

- 29 Zhao M. *et al.*, ‘Characterization of the atmosphere of the hot Jupiter HAT-P-32Ab and the M-dwarf companion HAT-P-32B’, *Astrophys. J.*, **796**, 115 (2014)
- 30 Gibson N. P. *et al.*, ‘The optical transmission spectrum of the hot Jupiter HAT-P-32b: clouds explain the absence of broad spectral features?’, *Mon. Not. R. Astron. Soc.*, **436**, 2974–2988 (2013)
- 31 Nortmann L. *et al.*, ‘The GTC exoplanet transit spectroscopy survey – IV. Confirmation of the flat transmission spectrum of HAT-P-32b’. *Astron. Astrophys.*, **594**, A65 (2016)
- 32 Mallonn M. & Strassmeier K. G., ‘Transmission spectroscopy of HAT-P-32b with the LBT: confirmation of clouds/hazes in the planetary atmosphere’. *Astron. Astrophys.*, **590**, A100 (2016)
- 33 Mallonn M. & Wakeford H. R., ‘Near-ultraviolet transit photometry of HAT-P-32 b with the Large Binocular Telescope: Silicate aerosols in the planetary atmosphere’, *Astron. Nachrichten*, **338**, 773–780 (2017)
- 34 Seeliger M. *et al.*, ‘Transit timing analysis in the HAT-P-32 system’. *Mon. Not. R. Astron. Soc.*, **441**, 304–315 (2014)
- 35 Each of the five telescopes in the MicroObservatory network are light-heartedly named after noted astronomers: *Amie* Jump Cannon, *Benjamin* Banneker, *Cecilia* Payne-Gaposchkin, *Donald* Menzel, and *Edward* Pickering.
- 36 *C-MUNIPACK*. Available at: <http://c-munipack.sourceforge.net/> (accessed 2020 April).
- 37 Eastman J., Gaudi B. S. & Agol E., ‘EXOFAST: A fast exoplanetary fitting suite in IDL’, *Publ. Astron. Soc. Pacific*, **125**, 83–112 (2013)
- 38 Eastman J., Siverd R. & Gaudi B. S., ‘Achieving better than 1 minute accuracy in the heliocentric and barycentric Julian dates’, *Publ. Astron. Soc. Pacific*, **122**, 935–946 (2010)
- 39 *MEOW* pipeline demonstration. Available at: <https://www.youtube.com/watch?v=fqVZho3fOkU> (accessed 2020 April).
- 40 Mandel K. & Agol E., ‘Analytic light curves for planetary transit searches’, *Astrophys. J.*, **580**, L171–L175 (2002)
- 41 Ford E. B., ‘Quantifying the uncertainty in the orbits of extrasolar planets’, *Astron. J.*, **129**, 1706–1717 (2005)
- 42 Ford E. B., ‘Improving the efficiency of Markov Chain Monte Carlo for analyzing the orbits of extrasolar planets’, *Astrophys. J.*, **642**, 505–522 (2006)
- 43 Ter Braak C. J. F., ‘A Markov Chain Monte Carlo version of the genetic algorithm Differential Evolution: Easy Bayesian computing for real parameter spaces’, *Stat. Comput.*, **16**, 239–249 (2006)
- 44 Auvergne M. *et al.*, ‘The CoRoT satellite in flight: description and performance’, *Astron. Astrophys.*, **506**, 411 (2009)
- 45 Carter J. A. *et al.*, ‘Analytic approximations for transit light curve observables and uncertainties’, *Astrophys. J.*, **689**, 499–512 (2008)
- 46 Fowler M. J. F., ‘Serendipitous observations of UCAC4 686-012519: a short period  $\delta$  Scuti pulsating star in Andromeda’, *Brit. Astron. Assoc. Variable Star Section Circ.*, no. 186, 33–38 (2020)

Received 2020 April 25; accepted 2020 July 1

## New members

### 2021 January 23

ALEXANDER Vernon, Stirling  
 ANDERSON Robert, Renfrewshire  
 BARRATT Michael, Wiltshire  
 BEECH Rebecca, Surrey  
 BENNETT Gillian, Worcestershire  
 BEZ-CRYER Isabella, Bath & North East Somerset  
 BEZUGLAYA Lena, Hammersmith & Fulham  
 BODDINGTON David, Berkshire  
 CERAVOLO Peter, British Columbia, CANADA  
 COCCIA Francesco, Napoli, ITALY  
 DAVIES Alun, North Yorkshire  
 DAVIS Anne, Kent  
 DRENNEN Debbie, Devon  
 DUBEY Kamlesh, Melaka, MALAYSIA  
 FELTON Miles, Cumbria  
 GEORGE Jodie, Poole  
 GREEN Tony, Coventry  
 GRICE Keith, Shropshire  
 HAMMOND James, East Ayrshire  
 HOULTON Nigel, Derbyshire  
 HUMBERSTONE Joseph, Conwy  
 Institute de Astronomia, Birmingham, USA  
 JONES-WELLS Owen, Dorset  
 KERESZTY Zsolt  
 KNAGGS Michael, Leicestershire  
 LEE Mark, Pembrokeshire  
 LEWIS Roger, Cardiff  
 MADHAVAN Jaswant, Franklin, USA  
 MAROTTA Michael, Texas, USA  
 MORRIS Brian, JERSEY  
 MURRAY Paul, Berkshire  
 OMER Michael, Gloucestershire  
 PATEL Pinakin, Cambridgeshire  
 PICKFORD Chris, Oxfordshire

PISTRITTO Davide, Bari, ITALY  
 PLATTS Chris, East Sussex  
 PLUME Christopher  
 RECORD Geoff, Derby  
 ROBINSON James, Wiltshire  
 ROWE Ken, London  
 SHADRACH David, Alpes-Maritimes, FRANCE  
 SMITH-SUAREZ Edward, Southwark  
 STEPHEN Neil, Edinburgh  
 THOMSON Matthew, London  
 TRUNLEY Harold, Lancashire  
 VAMPLEW Anton, Kent  
 WADE Thomas, Rotherham  
 WAREING Mark, Cumbria  
 YORK Stephen, Leicestershire  
 YOUNG Gordon, Essex

### 2021 March 31

AKTAS Sezer, İstanbul, TURKEY  
 ANDERSON Colin, Berkshire  
 ANNE Susan, Pembrokeshire  
 BOWSKILL Grant, Bedfordshire  
 BUCHHEIM Robert  
 BUCKLEY Derek, Dublin, IRELAND  
 CLARK Russell, Neath Port Talbot  
 CONWAY Dr Andrew, Glasgow  
 COOKE Martin, Alava, SPAIN  
 DAVIES Karl, Kent  
 DAVIS Mark  
 DOWNIE Gordon, Bath & North East Somerset  
 ELDRIDGE Colin, Western Australia, AUSTRALIA  
 EVANS Peter, London  
 FENTAMAN Arthur, Kent  
 FERNANDES Rollando, Leicestershire

FORBES Hilary  
 GREENHILL-HOOPER Mike, Occitanie, FRANCE  
 HODSON Brian, Lancashire  
 HOFFMANN Brian, York  
 JACKSON Leslie, Derby  
 KIISKINEN Harri, Jyväskylä, FINLAND  
 KIRK Adam, Nottinghamshire  
 KLAGES Peter, Shropshire  
 MALAMATENIOS David, Hertfordshire  
 MARSHALL James, Lincolnshire  
 MARSHALL Riya, Lincolnshire  
 McDONALD Gary, London  
 MCKEE Robert, Greater Manchester  
 MENZIES Kenneth, Massachusetts, USA  
 MILLS Peter, Norfolk  
 MORAN John, East Yorkshire  
 NEAL Mark, Berkshire  
 NELSON Peter, Liverpool  
 OWEN Kirsten, Hertfordshire  
 PARKES Dr Harry, Lewisham  
 PATTINSON David, Staffordshire  
 PEARSON Frank, Staffordshire  
 PEREZ SOLAR Christian, Angus  
 PYWELL Richard Francis, Cornwall  
 ROBERTSON Raymond, Brighton & Hove  
 ROMERO Luis, Barcelona, SPAIN  
 SILOW Fredrik, SWEDEN  
 SMITH Robert, Warwickshire  
 STONE Lynne, South Gloucestershire  
 STRICKLAND Stephen, West Yorkshire  
 TEMLETT Tom, Somerset  
 VALVASORI Adriano, Sala Bolognesa, ITALY  
 WARD Matthew, Dorset  
 WARDLEY Peter  
 WILBY Christopher, Bolton  
 WYKES Rory, Northamptonshire